

Available online at www.sciencedirect.com

SCIENCE @ DIRECT®

Sensors and Actuators B xxx (2005) xxx–xxx



Ethanol vapor detection in aqueous environments using micro-capacitors and dielectric polymers

Dennis L. McCorkle, Robert J. Warmack¹, Sanjay V. Patel²,
Todd Mlsna², Scott R. Hunter*, Thomas L. Ferrell

Department of Physics, University of Tennessee, 401 Nielsen Physics Building, Knoxville, TN 37996-1200, USA

Received 25 June 2004; received in revised form 30 November 2004; accepted 14 December 2004

Abstract

A technique for the measurement of ethanol concentrations in aqueous mixtures is reported, in which a permeable membrane is used to transport ethanol vapors to a microelectromechanical (MEMS) chemi-capacitor array. The fixed plate micro-capacitors were filled with a polymeric dielectric material, siloxane-fluoro alcohol (SXFA), whose dielectric constant increased upon absorption of ethanol vapor. Measurements of the mixture's liquid-phase concentration were made in the vapor-phase by sampling the saturated vapors through a hydrophobic, vapor permeable nanopore filter. The performance of these sensors was characterized over a range of ethanol/water mixture concentrations and flow cell temperatures. The limit of detection (LOD) for ethanol in water using the capacitive micro-sensors in the present arrangement was found to be 40 ppm.

© 2004 Elsevier B.V. All rights reserved.

Keywords: MEMS chemi-capacitor array; Dielectric polymers; Micro-capacitors; Alcohol sensing

1. Introduction

The measurement of ethanol concentrations in liquid environments is of considerable significance for a variety of purposes including ethanol production, industrial chemical processing, fuel processing and use, societal applications, and physiological research. A large number of commercial ethanol measurement systems are available for several of these applications, but in general, these systems are designed exclusively for vapor-phase measurements, operate at relatively high power levels, are bulky, and possess functionality that is more limited than required for a number of applications. Successful attempts [1,2] have previously been made to carry out selective bio-molecular sensing for ethanol

using alcohol-dehydrogenase, but this compound is an enzyme and has a limited lifetime, such that it is not suitable for many sensing applications. Another early bio-molecular sensor used methylotrophic micro-organisms [3], but micro-organisms are mainly applicable to fermentation monitoring and such sensors are not extant even in this case. Most ethanol sensors today rely upon the use of metal oxides and powders that catalyze the oxidation of ethanol and use electrochemical, electrical conductivity, or transduction by field-effect transistors [4–26]. Response times, power demands for metal oxide, and conducting polymer based sensors, or the need for oxygen in many sensors make them problematic. Nanoparticles and composites have been widely explored to aid in these methods of transduction, but power demand is a key problem particularly when sensor heating is required. Fiber-optic and luminescence-based sensors [27–32] also consume high power levels or are physically large. A major goal of the present study was to develop an ethanol micro-sensor of reduced size with low-power requirements and without the need for oxygen, while providing accurate measure-

* Corresponding author. Tel.: +1 8655748308; fax: +1 8655762661.

E-mail address: shunter@csot.com (S.R. Hunter).

¹ Oak Ridge National Laboratory, POB 2008, Oak Ridge, TN 37831, USA.

² Seacoast Science Inc., POB 130485, Carlsbad, CA 92013-0485, USA.

ment of physiologically significant ethanol levels in aqueous solutions.

Ethanol micro-sensors have been produced by several groups and include chemi-resistor [33,34], micro-capacitor [33–40] or micro-cantilever sensors [41–49]. Nanometer scale deflections of micro-cantilevers due to induced stress gradients across the cantilever structure have been sensed using optical readout techniques [50–52], but this configuration is not easily miniaturizable. Piezoelectric micro-cantilevers are more compact, but the zinc oxide piezoelectric layer is relatively thick, which results in a loss of sensitivity [49,53]. Additionally, the measurement of cantilever resonance frequency shift due to mass loading can be unreliable [54] particularly in liquid environments where the cantilever Q is low. Micro-cantilever systems using piezoresistive [55,56] or capacitive [57,58] sensing techniques have proven to be far more successful in providing compact low-power chemical sensing. Operation of micro-cantilever sensors in liquid environments can be problematic due to the need for insulation and where the cantilever bending response due to chemically induced changes in surface stress are usually much lower than for the corresponding vapor [59,60].

An alternative chemical sensing technique uses capacitive transduction, which offers low-power consumption and sensitive detection based upon changes in the dielectric constant or relative permittivity of the material between the capacitor plates [39,40,61,62]. Changes in the dielectric properties of the sensor lead to corresponding changes in the capacitance, and for the materials used in this study, the polar nature of alcohol causes the capacitance to increase over that of the unexposed sensor. The present capacitive sensors were fabricated using standard microelectromechanical (MEMS) micromachining techniques that enabled several miniature (sub-millimeter) capacitive sensors to be located on each sensor chip. An additional advantage of this fabrication technique is that the sensors are highly reproducible at the device and chip levels [40]. Major drawbacks of capacitive sensors are that the target molecule must cause a significant change in the sorbent material's dielectric constant to be detectable, and the sensor cannot be immersed directly in an ionic fluid that could reduce the parallel resistance across the capacitive sensor element to intolerable levels. We have overcome this limitation by performing gas-phase chemical sensing in liquid environments.

In this paper, we present results using a micro-capacitor ethanol sensor that samples the ethanol concentration in the saturated vapor from ethanol/water mixtures. The innovative features of this technique are the ability to accurately measure ethanol vapor concentrations in near 100% relative humidity environments with the sensor completely immersed in the aqueous environment if necessary. This is achieved by separating the vapor-sensing element from the liquid environment with a nanopore hydrophobic filter designed to have a high standoff pressure to the surrounding liquid. Capacitive-based sensing is ordinarily ruled out in the case of ionic fluids due to the deleterious effects of the ions on the impedance.

However, the use of membrane filters allows high impedance gaseous sensing while preventing the entrance of significant ion concentrations for extended periods of time. A further advantage of this technique is that the relative concentrations (moles/mole) of ethanol in water mixtures in the vapor and liquid equilibrium-phases for low ethanol concentrations are very different, being a factor of 5–10 higher relative concentration of ethanol in the vapor-phase as compared with the liquid-phase, depending on the liquid ethanol concentration and mixture temperature [63–65]. This results in much higher gas-phase ethanol concentrations in comparison with liquid-phase mixtures, and considerably improves the measured sensitivity detection limit for ethanol detection. When combining the inherent features of this sensor system (i.e. low-power, small form factor, and package size) with wireless telemetry, these sensor systems may find uses in a number of demanding applications including several medical (e.g. implantable sensors) and environmental (e.g. waste tanks and ponds, and well and ground water monitoring) applications.

In Section 2 below, we describe the micro-capacitor sensor system and the measurement apparatus and techniques. In Section 3, we present partition coefficient measurements for a number of polymers, from which the polymer siloxane-fluoro alcohol (SXFA) is chosen as the most promising dielectric fill material for detection of ethanol in near saturated water vapor mixtures. Capacitive sensor response data and analyses collected with various polymers for varying aqueous concentrations of ethanol are also presented. Finally, in Section 4, we summarize these measurements and draw conclusions from these analyses.

2. Experimental

2.1. Capacitive sensor elements

The capacitive sensor elements and detection and control electronics used to obtain the present measurements have been described previously [40,57,58,66]. The sensors in the present study are composed of micromachined parallel-plate capacitors (Fig. 1) with a fixed plate separation that are fabricated with multiple capacitive sensors on each sensor chip. A photograph of a fabricated sensor chip containing eight capacitive sensors used in these studies is shown in Fig. 2. This multiple sensor arrangement allows reproducibility studies, multi-polymer response studies, and polymer filling studies to easily be performed on a single chip.

The sensor chips (Fig. 2) used in the present studies were fabricated in the Multi-User MEMS Process (MUMPs) at MEMSCAP, Durham, NC. These chips measured 5 mm × 2 mm and contained eight circular parallel-plate capacitors that could be coated or filled with varying amounts of the polymer dielectric material, or each sensor element could receive a different coating. The capacitor plates were made of conductive polycrystalline silicon consisting of a 0.5- μ m thick bottom plate resting on the substrate, an air

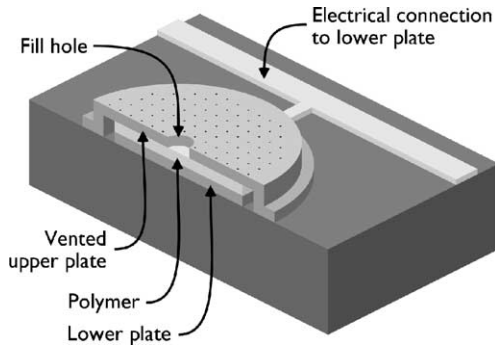


Fig. 1. Schematic diagram of the micromachined parallel plate capacitive sensors used in the present studies. The top plate of the capacitor contains a large fill hole, which is used to deposit the polymer dielectric material, and an array of smaller holes to allow vapors to interact with the polymer fill material.

gap that was filled with polymer subsequent to the MEMS fabrication process, and a 2- μm thick ventilated top plate. The circular capacitor plates were 550 μm in diameter with a 125- μm diameter central dielectric fill hole (Fig. 1), with a 2- μm gap and an unfilled capacitance of about 0.8 pF.

To minimize the possible flexing of the top plate when the polymer swelled due to absorption of the ethanol or water vapor, the top plate was anchored to the substrate with posts (5 μm^2) at approximately 60 μm intervals. The top plate also had an array of 3- μm^2 etch holes separated by about 30 μm . These holes were required for removal of a sacrificial silicon dioxide layer during chip fabrication, and also to allow analyte vapors to pass through the top plate to interact with the underlying polymer dielectric material during operation.

2.2. Detection electronics

The signal detection sensor control electronics were fabricated at the Oak Ridge National Laboratory, and have been described in previous publications about capacitive cantilever-based sensors [40,57,58,66]. The signal detection electronics are identical to those used in the cantilever studies as both devices had similar capacitances and dynamic ranges. Briefly, a charge/discharge readout circuit [57,58]

measured the capacitance of each sensor array using a 10 kHz charge/discharge drive voltage, and produced a corresponding ac output voltage V_{out} :

$$V_{\text{out}} = \Delta V_{\text{osc}} \frac{C_{\text{sensor}}}{C_{\text{feedback}}} \tag{1}$$

where ΔV_{osc} is the amplitude of the oscillator drive voltage, C_{sensor} the capacitance of the capacitive sensor, and C_{feedback} is the reference feedback capacitance. The output voltage is recorded by a sample-and-hold circuit that provides a dc reference voltage, V_R , minus the amplitude of V_{out} , (i.e. the observed signal $V_S = V_R - V_{\text{out}}$). Thus, decreases in the output voltage of the circuit when the capacitors are exposed to the alcohol/water mixtures correspond to increases in the capacitance of these capacitive sensors.

The sensor chips were mounted directly on a daughterboard (Fig. 3) with the custom sensor preamplifier integrated circuit. The daughterboard was in turn mounted on a motherboard containing the drive oscillator and power supply. The average measured noise voltage for several unfilled micro-capacitor sensors was $\Delta V_{\text{noise}} \approx 0.15$ mV. This value corresponds to an uncertainty in the measured capacitance of $\Delta C \approx 0.075$ fF, or a smallest measurable capacitance change of 0.23 fF with a signal-to-noise ratio of 3. This is in agreement with previously measured sensitivity limits for similar sensors and electronics [40].

The relative permittivity $\epsilon_{\text{polymer}}$, or dielectric constant of the polymer dielectric is simply the ratio of the polymer filled to unfilled sensor capacitance, or equivalently, by the ratio of V_{out} for filled and unfilled capacitors. This analysis procedure was used to obtain the value of the dielectric constant for SXFA given in Table 1.

2.3. Polymer dielectric fill material

The polymeric dielectric materials used in the capacitive sensors studies were dissolved in a solvent (typically chloroform for these studies) and were deposited as droplets onto the sensor capacitors with a manually positioned piezoceramic inkjet head (Microfab Technologies MJ-ABP-03030- or

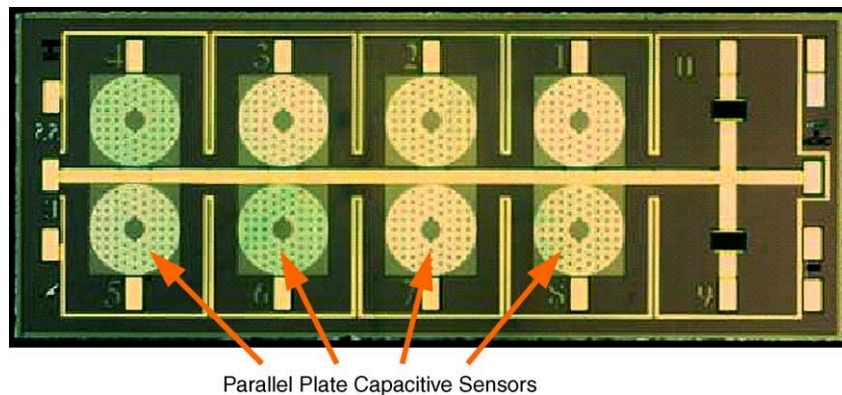


Fig. 2. Photograph of a micromachined sensor chip containing eight circular micromachined capacitive sensors and two on-chip temperature sensors.

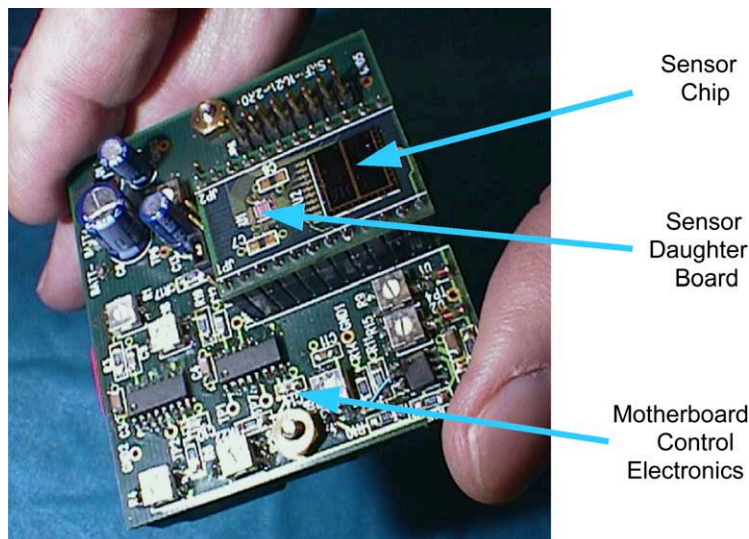


Fig. 3. Vapor sensor electronics package showing the sensor chip, the daughter printed circuit board containing the sensor preamplifier, and the motherboard containing the control and multiplexing and the A/D electronics.

50- μm dispenser with Microfab JetDrive inkjet controller). The inkjet head was positioned over the sensor chip using a Leitz mechanical micromanipulator to deposit individual droplets (30–50 μm diameter) of the polymer solution with repetition rates of 1–100 Hz, and which dried in about 1 s. Solutions were mixed to a concentration that did not clog the inkjet nozzle (indicating that the solution was too concentrated) or wash away previously deposited polymer (too dilute). The solution concentrations were in the range 0.1–2% by weight of polymer in the solvent.

The eight sensor capacitors on each chip (Fig. 2) were filled with varying amounts of polymer material, and the

capacitance and dielectric constant of each of these sensors was monitored to estimate whether the dielectric material had filled the entire gap of the capacitors. Typically, 10,000 drops with a diameter of 30 μm using solutions containing 0.1% dissolved polymer were required to fill the capacitors. With 50- μm diameter drops, around 2000 drops were required to fill the capacitors. Since the droplets were so small, most of the solvent evaporated before the next drop landed. Coatings were typically applied to seven “signal” capacitors, leaving one uncoated capacitor. The uncoated capacitors did not respond to chemical exposures or changes in relative humidity, flow rate or temperature.

Table 1

Literature values for the dielectric constants and present measured partition coefficients for several polymers

Polymer	Abbreviated name	Dielectric constant[40]	Measured K (water)	Measured K (ethanol)
Siloxane/fluoro alcohol	SXFA	7.3, 4.14 \pm 0.03*	337	992
Polyethylene-co-vinylacetate	PEVA-18	4.1	296	114
Polyethyleneimine	PEI		18300	2540
Poly(dimethyl(siloxane)-co-(3-aminopropyl)methylsiloxane)	DMS-APM		51	94
Polydimethyl siloxane	PDMS	2.5	160	83
Polyurethane	PU		443	471
Poly(etherurethane)	Tecoflex		627	503
Poly(ethyleneoxide)	PEO		30000	213
	Novolac		13300	273
Cyanopropyl methyl phenylmethyl silicone	OV-225	11	108	217
Dicyanoallyl silicone	OV-275	33	964	389
Phenyl methyl silicone	OV-17		312	593
Polymethylmethacrylate	PMMA		717	731
Polyepichlorohydrine	PECH	7.4	132	221
	Polycarbonate		212	141
Analyte				
Water		80		
Ethanol		25.3		

* Present measured value.

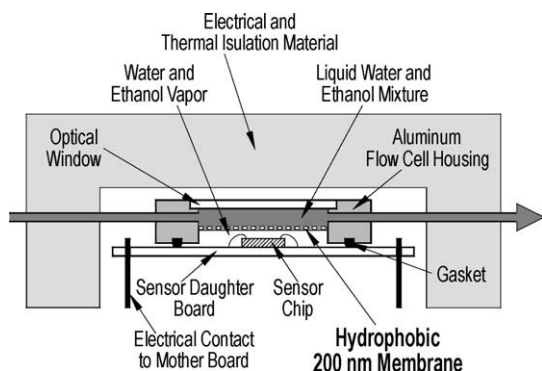


Fig. 4. Diagram of the fluid flow cell used to flow the aqueous ethanol/water solution over the hydrophobic filter membrane. Ethanol and water vapor pass through the filter and are absorbed by the polymer dielectric material in the microsensors capacitive elements.

2.4. Flow cell design

A unique aspect of the present studies is the capacitive sensor response to the varying ethanol concentrations and temperatures, which was measured in an atmosphere containing a relative humidity level of near 100%. This allowed simulation of the sensor response when completely immersed in liquid water environments, and was achieved in the present studies by fabricating a two compartment aluminum flow cell separated by a 200 nm pore size hydrophobic membrane filter (GE Osmonics [67]) (Fig. 4) to separate the liquid- and vapor-phases of the ethanol/water mixtures. The filter was held in place by a rigid support holder (not shown in Fig. 4), which prevented it from flexing during changes in cell temperature and liquid flow rates. Unique features of these membranes include their high permeation rates for air and other gases, along with their ability to withstand water pressures up to two atmospheres without wetting or leakage, and their relative inertness in most common solvents [67]. The flow cell was positioned over the capacitive sensor chip located on the sensor daughterboard (Fig. 3) and clamped in place to form a hermetic seal between the flow cell and printed circuit board using the gasket shown in Fig. 4. This allowed us to form a sealed, vapor-phase chamber above the sensor chip, 12 mm in diameter and approximately 1 mm in height.

A schematic diagram of the experimental flow and temperature control apparatus is shown in Fig. 5. Mixture flow control valves and a peristaltic pump (ColeParmer No. 7335-30) maintained constant flow rates from two vessels containing laboratory deionized water (Barnshead NANOpure water system) and ethanol/water mixtures. Ethanol was obtained from AAPER Alcohol and Chemical Co. with a stated concentration of 95%, and prediluted with the deionized water to a specific concentration before each set of measurements. Ethanol concentrations were determined by mixing a known volume of pure alcohol in a known volume of the deionized water and agitating to ensure complete mixing in the container. As shown in Fig. 5, the fluid flow through the flow cell was then established by switching the fluid from either

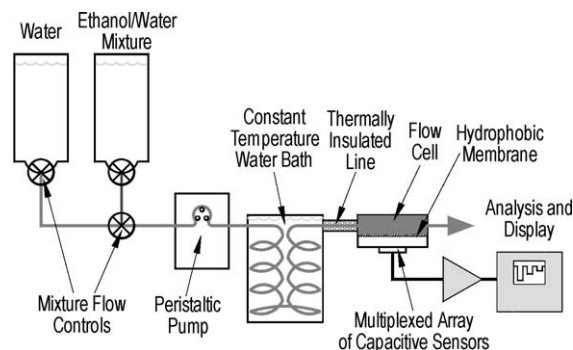


Fig. 5. Diagram of the apparatus used to control the concentration and temperature of the ethanol/water mixtures.

of two containers containing pure water and the premixed ethanol/water (with concentrations in the 0.1–2.0% range) mixtures into the 1 mm internal diameter stainless steel line flowing into the flow cell. A three-way valve, with a switching time under 1 s, was used to switch between the two fluid containers. The pure water or ethanol/water mixtures were passed through a constant temperature water bath (VWR Scientific Products No. 1167), and the short output line from the bath was thermally insulated and used as the input to the flow cell. The flow times from the switching valve to the sensor cell were around 10 s, and the purge time for the flow cell was around 1–2 s. In this situation, the transition time from no alcohol to the dilute alcohol mixtures in the flow cell is around 1–3 s and is negligible in comparison with the filter/sensor response time (1 to several minutes). The flow cell was covered in thermal and electrical insulating material to minimize temperature fluctuations and induced electrical noise in the sensor chip.

2.5. Polymer partition coefficient measurement technique

There are several polymer related variables that affect the performance of these capacitive sensors in the present application. The polymers must possess a low dielectric coefficient relative to that of ethanol, thereby maximizing the change in capacitance when exposed to the ethanol mixtures, and a high partition coefficient relative to water. The partition coefficient, K , is a thermodynamic parameter that measures the equilibrium distribution of vapor between the gas-phase and the sorbent-phase; i.e. [68]:

$$K = \frac{C_s}{C_v} \quad (2)$$

where C_s and C_v are the concentrations of the vapor in the sorbent- and vapor-phase, respectively. The sorbent-phase is composed of the polymer material between the capacitor plates, which absorbs the analyte thereby changing K and thus the sensor capacitance.

The partition coefficients for a variety of polymeric materials, which had potential for use in the capacitive sensors,

were obtained using quartz crystal microbalance (QCM) sensors in a dedicated measurement system. The advantage of these sensors is that they are relatively simple devices to operate producing a quasidigital frequency signal with good noise and interference rejection and low rates of signal drift. The major disadvantages of these types of sensors in the present alcohol measurement application is the physical size limit of the devices (for physiological applications, the sensors must have sub-millimeter dimensions), and the inherent sensitivity limits of around 0.1 ng/mm^2 for these sensors [69]. They proved, however, to be excellent sensing devices to quickly screen likely candidate polymers for use in the capacitive sensors.

The partition coefficient measurement technique using these sensors is as follows. Several QCMs ($f_0 = 6 \text{ MHz}$ QCMs manufactured by International Crystal Manufacturing) were spray coated with low-concentration polymer solutions while the resonant frequency change, Δf_p , in the QCM was monitored (HP model no. Z-53131A Universal Counter). Typically, the polymer material was deposited on the QCM until a measured frequency change of $\Delta f_p = -5 \text{ kHz}$ was registered. Up to four QCMs were then placed in a hermetically sealed chamber and ethanol/nitrogen and water vapor/nitrogen mixtures were flowed through the chamber. The temporal change in the QCM resonant frequency was recorded until the response became invariant with time, indicating that vapor sorption/desorption equilibrium had been achieved. The mass of the deposited material, Δm_p , can be obtained from the Sauerbrey equation [69], which gives a direct proportionality between the measured frequency change, Δf_p , and the deposited mass, Δm_p , on the active area of the crystal.

Up to four of the polymer coated QCMs could be mounted and measured in a hermetically sealed test chamber heated and temperature stabilized by a Lytron heat exchanger and a VWR Model 1167 Programmable Liquid Circulator. Water vapor mixtures were created by flowing a stream of nitrogen, at atmospheric pressures, through a gas bubbler containing pure deionized water at 25°C . This saturated water vapor stream was passed through a computer controlled MKS mass flow controller and was mixed with a second stream of dry nitrogen whose flow rate was controlled by a second mass flow controller. Ethanol/nitrogen mixtures were formed in a similar manner except that the saturated ethanol/nitrogen mixtures were formed by flowing nitrogen through a temperature controlled cell containing purified alcohol. Known concentrations of water vapor and ethanol in nitrogen were obtained by adjusting the flow rates of the two vapor streams (either water or ethanol vapor saturated mixtures and pure nitrogen) entering a mixing chamber. The resultant vapor mixture was then passed to the test chamber and allowed to interact with the QCMs.

The change in the resonant frequency, Δf_a of the QCMs due to the absorption of the analyte was monitored until equilibrium was reached where analyte absorption and desorption on the polymers were balanced. The relative change in resonance frequency due to analyte absorption is found from

the Sauerbrey equation [69] to be equal to the relative mass change, i.e.:

$$\frac{\Delta f_a}{\Delta f_p} = \frac{\Delta m_a}{\Delta m_p} \quad (3)$$

where Δm_a is the mass of the absorbed analyte and Δf_a is the change in QCM resonance frequency due to the absorbed analyte.

Consequently, the partition coefficient for the analyte/polymer pair is related to the change in frequency (or mass) by the following:

$$K = \frac{\Delta f_a}{\Delta f_p} \cdot \frac{\rho_p}{C_v} \quad (4)$$

where ρ_p is the density of the polymer. Performing a series of Δf_a measurements as a function of the known mass concentration of the analyte, C_v , allows the partition coefficient for the particular polymer/analyte combination to be obtained at a given temperature.

3. Results

3.1. Partition coefficients

A series of partition coefficient measurements were performed on a range of polymers listed in Table 1. These polymers were chosen based on the literature values (e.g. [40,68]) of their dielectric properties, vapor pressures, etc. The ideal polymer for use in the present application must possess a low dielectric constant (much less than that of ethanol), a high partition coefficient for ethanol, preferably a high specificity to ethanol over water or other potential interferents, and for ease of deposition, be a viscous fluid or solid readily soluble in common non-reactive solvents. The polymers chosen for this study based on these requirements are listed in Table 1, along with their abbreviated names and dielectric strengths where known.

These polymers and their synthesis precursors were purchased from Polysciences Inc. (Warrington, PA), Scientific Polymers Inc. (Ontario, NY), Gelest Inc. (Morrisville, PA), or Sigma–Aldrich (St. Louis, MO). The polymers Novalac, Tecoflex, and polycarbonate were obtained from Dow Chemical, Thermetrics Polymer Products, and Rohm and Haas, respectively. The fluoroalcohol SXFA was synthesized in-house from methods found in the literature [40,70]. Ultra high purity nitrogen (UHP, 99.999%, <10 ppm water vapor) for the partition coefficient measurements was obtained from Air Liquide.

A series of QCM resonant frequency response measurements were performed on each of the chosen polymers as a function of water and ethanol vapor concentration in UHP nitrogen. An example set of response measurements for the SXFA polymer with the ethanol/nitrogen and water vapor/nitrogen mixtures is shown in Fig. 6. As the concentration of water or ethanol increases, the QCM resonant frequency

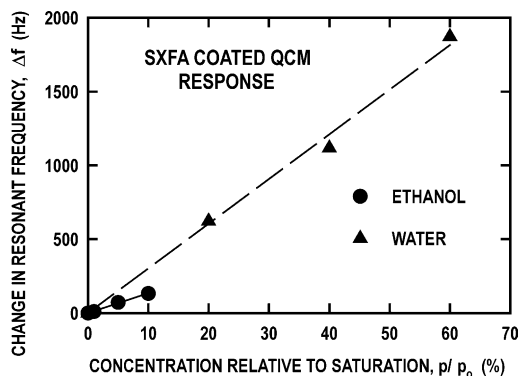


Fig. 6. The averaged change in resonance frequency for four QCM sensors as a function of the concentration of ethanol and water in air at room pressure and 25 °C. The QCM in this example was coated with SXFA.

decreases due to additional mass loading by absorption of the ethanol or water vapor. These and similar results for other polymers indicated that the observed change in resonance frequency was linear with vapor concentration over the range of concentrations used in these measurements. The partition coefficients, K , for both ethanol and water vapor were obtained from these measurements using the analysis given above, and these values are given in Table 1 for a number of polymers. There is an almost three orders of magnitude range in K -values for water vapor and a much smaller 30-fold range in values for ethanol. Based on the polymer requirements listed above, the best polymer choice for the ethanol vapor measurements was found to be SXFA, due to its moderately large value for K , which was higher than that for water vapor, its comparatively low dielectric constant (Table 1), and its ease of use in the capacitance measurements.

3.2. Responsivity measurements

After the micro-capacitors were filled with SXFA (or other polymer under study), the relative permittivity, $\epsilon_{\text{polymer}}$, for each of the filled sensors was calculated using a separate gas flow cell and capacitance measurement system (similar to that outlined in Ref. [40]). The present measured value of $\epsilon_{\text{polymer}}$ for SXFA is given in Table 1 in comparison with the literature value [40]. The differences in the measured $\epsilon_{\text{polymer}}$ values reflect the differences in the dielectric properties of the custom fabricated samples. These measurements were used to verify that the gap between the plates in each of the capacitive sensors was filled with the polymer and that the calculated $\epsilon_{\text{polymer}}$ values were the expected values. These sensor chips were then mounted on the fluid-flow-cell daughterboard (Fig. 3), the fluid cell reassembled, and the individual micro-capacitor sensor responses recorded as a function of time, ethanol/water vapor mixture concentration, and flow cell temperature.

Output responses for several of the micro-capacitor sensors located on one sensor chip are shown in Fig. 7 for a range of ethanol concentrations in water at a water bath temperature of ~24 °C. The initial temporal dependence of the measured

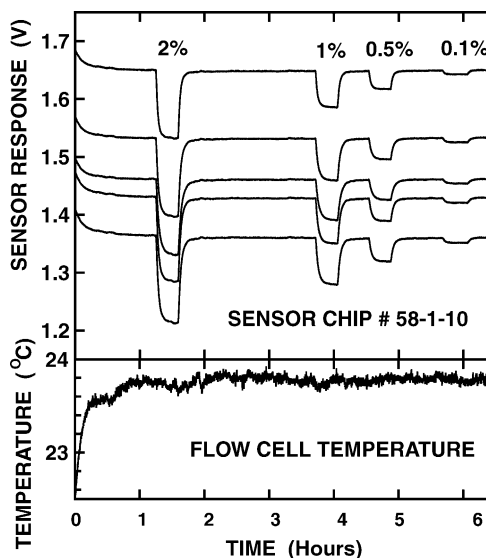


Fig. 7. Example sensor response measurements for several of the SXFA coated micro-capacitor sensors located on one sensor chip, as a function of time and ethanol concentration from 0.1 to 2.0% in water at 25 °C. Also shown is the sensor temperature measured with a temperature sensor located within the flow cell.

flow cell temperature is also included in Fig. 7, and shows that the sensor response is also a function of fluid temperature; the higher the temperature the larger the capacitance (i.e. the lower the sensor output voltage), primarily due to the increased uptake of the ethanol at the higher temperatures. The equilibrium sensor output responses at each of the ethanol concentrations were used to calculate the change in sensor capacitance, $\Delta C/C_{\text{sensor}}$, due to the change in ethanol concentration from Eq. (1), i.e.:

$$\frac{\Delta C}{C_{\text{sensor}}} = \frac{\Delta V_{\text{out}}}{V_{\text{out}}} \tag{5}$$

where C_{sensor} and V_{out} are the sensor capacitance and sensor voltage (V_{out} in Eq. (1)) in the humid environment, respectively.

Typical sensor response curves are plotted in Fig. 8 as a function of the ethanol concentration for five of the sensors

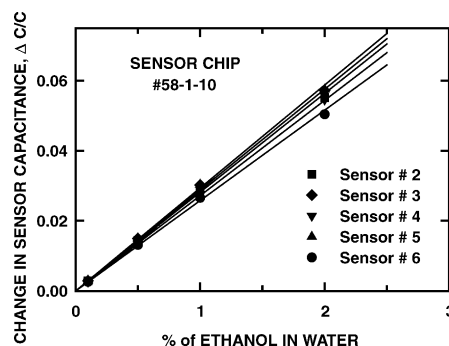


Fig. 8. The change in the SXFA coated sensor output capacitance as a function of the ethanol concentration obtained from the measurements shown in Fig. 7 for several of the individual micro-capacitor sensors located on one sensor chip.

located on the sensor chip. Similar measurements have been made with a flow cell that did not contain the hydrophobic filter. The sensor response under these conditions was essentially identical to that obtained with the hydrophobic filter, and consequently, the presence or absence of the filter has a negligible effect on the sensor sensitivity and response time as a function of the temperature or alcohol concentration. The relative change in capacitance is observed to vary linearly over the 0.1–2.0% range of concentrations measured in these experiments.

The sensor capacitance increases with increasing ethanol concentration, which is consistent with the QCM measurements presented in Fig. 6 where the change in resonant frequency (and hence mass loading) increases with ethanol concentration. The increase in capacitance is caused by additional sorption of ethanol by the SXFA, increasing the effective dielectric constant of the SXFA. Displacement of the relatively high dielectric constant water ($K=80$) by ethanol ($K=25.3$) would have led to a reduction in measured capacitance, and hence relative dielectric constant of SXFA, with increasing ethanol concentration. These results indicate that the ethanol sorption in the SXFA dielectric material, and the resultant change in dielectric constant, is a linear function of the ethanol concentration over this concentration range and is again consistent with the QCM measurements shown in Fig. 6.

3.3. Temperature dependence

A second set of measurements of the sensor response to changes in the flow cell operating temperature is shown in Fig. 9 for a 2.0% ethanol mixture, along with the

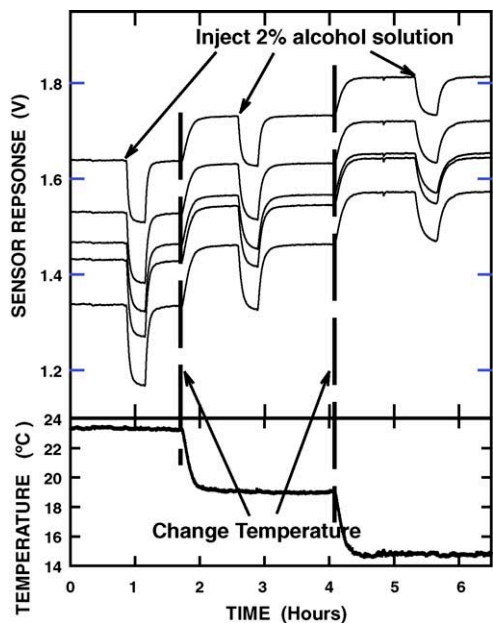


Fig. 9. Output response for several micro-capacitor sensors as a function of time for injections of 2.0% ethanol/water solutions, at three different nominal sensor temperatures.

measured temporal change in the flow cell temperature. These results show that the sensor capacitor response time when exposed to the alcohol solutions, τ_1 , and the capacitor response-time when the alcohol is purged from the sensor, τ_2 , along with the equilibrium change in capacitance, $\Delta C(\text{eq})/C_{\text{sensor}}$, are strong functions of the flow cell temperature and sensor temperature. The measured temporal sensor response appears to follow an exponential response when exposed to rapid changes in the ethanol/water mixture concentration, i.e.:

$$\frac{\Delta C(t)}{C_{\text{sensor}}} = \frac{\Delta C(\text{eq})}{C_{\text{sensor}} \exp(-t/\tau_{1,2})} \quad (6)$$

Eq. (6) is applicable under the following assumptions. First, there is a step function change in the alcohol concentration in the fluid flowing through the flow cell with a rise time that is much smaller than the response time of the sensor system. Second, that one rate of change mechanism in the sensor response dominates the sensor response time. Under these circumstances, the output response can be approximated by the standard exponential response function given in Eq. (6). As to the first point, the transition time for changes in alcohol concentration in the cell is of the order of 1–3 s as noted in Section 2.4, while the observed sensor response time is one to several minutes (Fig. 10), so this condition is satisfied. Secondly, the sensor response is dominated by the diffusion of the alcohol vapor into the polymer filled capacitor. The permeation time through the hydrophobic filter is negligible in comparison with the diffusion response time. This was readily observed by removing the hydrophobic filter and orienting the cell such that the sensor observes the head space above the liquid in the flow cell, being careful not to allow liquid to make contact with the capacitive sensors. Under these circumstance, the observed sensor response times with and without the filter were essentially identical, showing that the sensor response time is dominated by the polymer diffusion times in the sensor capacitor.

The sensor response data shown in Fig. 9 were taken at 10-s intervals and plotted over a time periods up to several

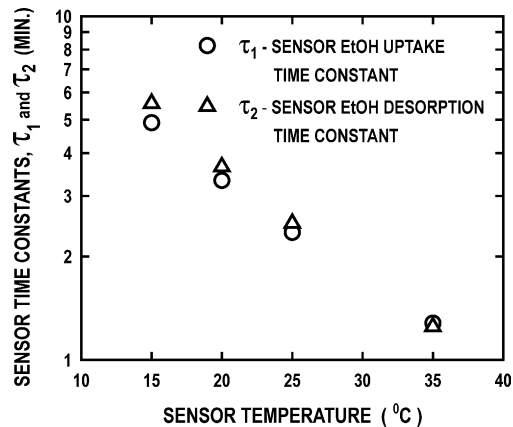


Fig. 10. The calculated sensor response time as a function of flow cell temperature for a 2.0% ethanol solution.

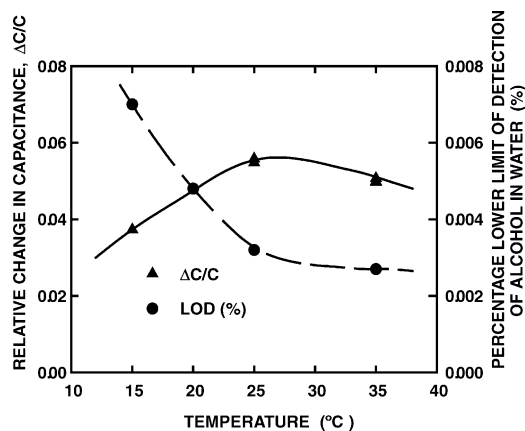


Fig. 11. The calculated change in capacitance as a function of temperature obtained from the measurements in Fig. 10 and other similar data over the temperature range from 15 to 35 °C. Also shown is the estimated lower limit of alcohol detection (LOD) obtained from these measurements, which approached 0.027% at the higher fluid temperatures.

hours. The response-time estimates were made by extracting segments of these data files for time periods around the time that the changes in alcohol concentration occur (periods of several minutes), and replotted. These data were then fitted to Eq. (6) and the time constant adjusted until a best fit to the data is obtained. The equilibrium τ_1 and τ_2 values, along with the $\Delta C/C_{\text{sensor}}$ values calculated for the 2.0% ethanol mixtures are plotted in Figs. 10 and 11, respectively, as a function of the flow cell temperature. The response-times, τ_2 , when the ethanol is purged from the flow cell are slightly longer than τ_1 at the lower cell temperatures, but they are essentially identical at temperatures above 30 °C. It is interesting to note that the response times have an approximate exponential dependence on sensor temperature with a characteristic temperature constant of ≈ 15 °C for exposures to the ethanol mixtures, and ≈ 13 °C characteristic temperature for cell purging. The reasons for this dependence have not been studied in this project.

These results show that the response time rapidly decreases with increasing sensor temperature, primarily due to the decreased ethanol diffusion times in the soft semi-liquid SXFA polymer dielectric material, leading to rapid vapor sorption/desorption equilibrium conditions at the elevated temperatures. In contrast, the change in the sensor capacitance initially increases with temperature for the 2.0% ethanol concentrations but, at temperature around 25–30 °C, the relative change in capacitance begins to decrease. A possible explanation for this observation is that at the lower temperatures, the vapor pressure above the ethanol/water mixtures rapidly rises with temperature leading to increasing sensor loading with temperature, and hence larger changes in the dielectric constant and concomitant increases in sensor capacitance. At higher temperatures, the rate of increase in vapor with temperature decreases along with the ethanol vapor/liquid partition coefficient with increasing temperature, leading to slightly reduced $\Delta C(\text{eq})/C_{\text{sensor}}$ values. Similar

results were observed for the 0.1% concentration measurements.

3.4. Sensitivity analysis

Sensitivity limits for the present micro-capacitive sensors and supporting electronics have been found by performing a series of measurements with a 0.1% concentration of ethanol/water mixtures. Measurements obtained for two sensors on the same chip (Fig. 2) are plotted on a magnified scale in Fig. 12 where the response of one of the sensors has been renormalized and overlaid on that of the other sensor. The renormalization was done by subtracting the voltage difference between the raw sensor output responses from one of the sensor response curves, similar to those shown in Figs. 7 and 9, at 80 min into the sensor response measurements (approximately half way through the measurement sequence) and plotting the resulting response along with that from the other sensor. This was done to show the high degree of correlation in the signal and noise responses obtained between these two sensors (and all the other coated sensors on the chip). Also plotted in the figure is the temporal difference signal between the normalized responses of these two sensors along with the flow cell temperature, which are plotted to highlight the sources of noise in the present measurements.

The estimated lower limit of detection (LOD) for the detection of ethanol in water mixtures using these micro-capacitive sensors has been calculated using an rms signal-to-noise ratio of 3. The signal and noise estimates were made by averaging the observed voltage measurements, with and without alcohol, over 10 min intervals (approximately 60 individual voltage measurements were obtained during successive 10 s signal sampling integration intervals) when an equilibrium response had been obtained for sensors with the greatest change in capacitance, corresponding to full or nearly filled

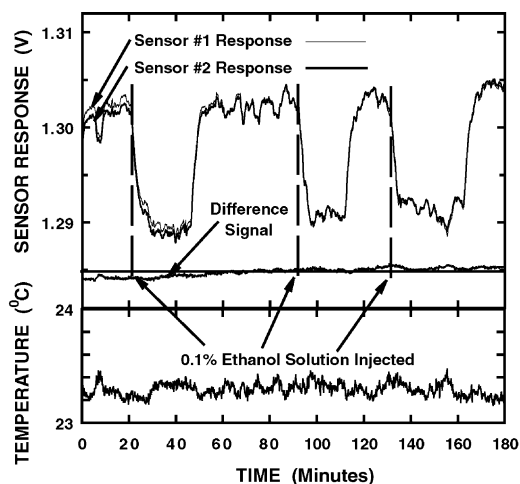


Fig. 12. The renormalized sensor response measurements for two of the micro-capacitors as a function of time for several injections of 0.1% ethanol/water solutions at 23.3 °C. Also shown is the difference signal between these responses, and the flow cell temperature.

gaps. These measurements were repeated several times for several injections of alcohol to check for repeatability. Measurements were also obtained for several individual sensors on the chip (up to six for the present chips) and observed for response consistency. In this manner, our measurements indicate an LOD for alcohol ≈ 40 ppm (v/v ratio). This detection limit implies an LOD ≈ 32 ng/ml of EtOH in water, which is comparable with an LOD = 16 ppm obtained using similar micro-capacitive sensors [40], but in a purely vapor-phase environment without a filter or membrane in the measurement chamber. Similar LOD values are achievable in the present experiments with improved regulation of the flow cell temperature.

Improved sensor sensitivity can be demonstrated by observing the sensor response and temperature plots shown in Fig. 12. These results indicate that although there is a small gradual long-term drift in the difference signal between these two sensors, most of the temporal noise is identical, with the largest contribution being correlated with the recorded fluctuations in the flow cell temperature. Small increases in cell temperature lead to lower sensor output voltages (i.e. higher values for ΔV_{out} and thus ΔC) in agreement with the temperature measurements presented in Figs. 9 and 11.

The temporal change in the capacitance of sensor #1 has been calculated using Eq. (1) and the temporal response voltage shown in Fig. 12 when the sensor was exposed to the 0.1% alcohol concentration. The value of C_{feedback} in Eq. (1) was 1 pF, $V_{\text{osc}} = 2$ V, and dc reference voltage $V_{\text{R}} = 4$ V. The temporal change in sensor capacitance is shown in Fig. 13 along with the calculated sensor capacitance where the effect of temperature on the sensor response has been minimized by subtracting the temperature signal from the sensor response signal using a multiplication and offset correction factor designed to minimize the influence of temperature variations on the sensor response. The response curves with and without the temperature correction shown in Fig. 13 indicate that the major excursions in the sensor response are due to changes in

the fluid flow cell temperature, creating increases in ethanol and water vapor concentration with increasing temperature and leading to increases in the sensor capacitance.

Improved control of the flow cell and liquid ethanol/water mixture temperatures would have considerably reduced the uncertainty in these measurements, and consequently the LOD value for the detection of ethanol using these micro-capacitive sensors. Normalization of output against reference sensors on the same chip should also improve the signal-to-noise considerably. Finally, the present measurements imply that the dynamic range with linear sensor response is at least 500:1, which is more than adequate for a number of industrial, environmental and medical monitoring applications.

4. Conclusions

We have shown that the present capacitive sensors, filled with SXFA as the dielectric material, possess LOD values around 40 ppm for ethanol on near saturated ethanol/water vapor mixtures over the temperature range from 15 to 35 °C. We have also shown that the sensitivity limit improves over this range of sensor temperatures due primarily to an increase in the change in capacitance with increasing temperature (Fig. 12) when the sensor is exposed to the ethanol/water solutions. The advantages of using SXFA as the dielectric material in the present micro-capacitive sensors for sensing ethanol are the large ethanol/SXFA partition coefficient in comparison with water/SXFA and the comparatively low dielectric constant of this material in comparison with that for ethanol (Table 1). The increased ethanol sensitivity at higher temperatures is due at least in part to the increasing vapor/liquid equilibrium ratio of the ethanol/water mixtures with increasing temperature [64,65], even though the saturated vapor pressure for water varies from 1.71 to 5.32 kPa over this temperature range [71], and that the partition coefficient, K , for the SXFA polymer for ethanol is approximately three times that of water (Table 1) at 25°. The sensitivity of the capacitive sensors is presently limited by electrical noise and temperature regulation of the flow cell and sensor chip, and improvements in these areas will considerably improve threshold limits.

We have also demonstrated with the fluid/vapor flow cell experiments reported in this paper that vapor-phase sensing of the presence of low concentration volatile analytes in aqueous mixtures is feasible using a highly permeable hydrophobic nanopore filter to separate the gas and liquid-phases. The advantages of this arrangement are that for a number of volatile organic compounds, the vapor/liquid equilibrium ratios are considerably in excess of one at low analyte concentrations (the equilibrium ratio is close to 10 over the concentration range of up to 2% for the ethanol/water mixtures in this study) [64,65]. Additionally, several types of chemical sensors have greater sensitivities in vapor-phase measurements as opposed to liquid-phase measurements [59,60]. These observations lead to much higher sensor sensitivities than would be expected based on the liquid analyte concentrations. Additional

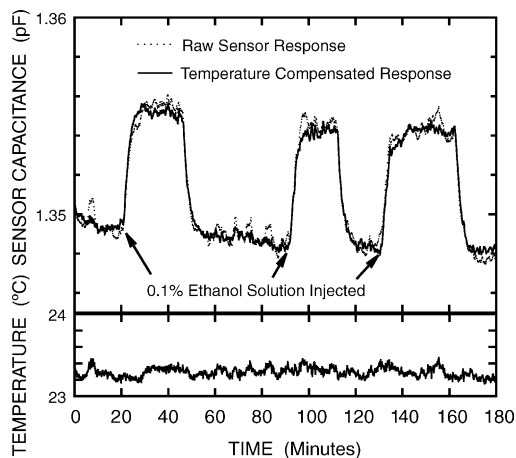


Fig. 13. The temporal variation in sensor 1 capacitance, calculated using Eq. (1) using the uncompensated and temperature compensated sensor response shown in Fig. 12.

advantages of the present micro-capacitive sensors are that we have shown that they perform well in near saturated water vapor environments, have a large and linear dynamic range for ethanol concentrations in water up to 2%, and response times from one to several minutes depending on the sensor temperature. This leads to the possibility of fabricating completely self-contained, miniaturized, remotely-operated sensors which are completely immersible in aqueous environments. There are many process monitoring, medical and environmental applications requiring sensors with these unique characteristics.

Acknowledgements

We would like to thank Oak Ridge National Laboratory for their support and use of their facilities, particularly J.E. Hardy. The readout electronics were designed by C.L. Britton and a number of colleagues at ORNL. Funding for this project came primarily from the National Institute of Alcoholism and Alcohol Abuse under Contract No. N01AA23012

References

- [1] S. Miyamoto, et al., Development of an amperometric alcohol sensor based on immobilized alcohol dehydrogenase and entrapped NAD⁺, *Biosens. Bioelectron.* 6 (7) (1991) 563–567.
- [2] A. Ramanavicius, et al., An oxygen-independent ethanol sensor based on quinoxaline alcohol dehydrogenase covalently bound to a functionalized polypyrrole film, in: *Progress in Colloid and Polymer Science*, Springer-Verlag, Heidelberg, 2000, 143–148.
- [3] J.-C. Chen, T.J. Naglak, H.Y. Wang, An amperometric alcohol sensor based on chemically permeabilized methylotrophic micro-organisms, *Biotechnol. Prog.* 8 (1992) 161–164.
- [4] P.P. Tsai, I.-C. Chen, M.H. Tzeng, Tin oxide (SnO_x) alcohol sensor from metal organic decomposed (MOD) thick film, *Sens. Actuators B Chem.* 14 (1–3) (1993) 610–612.
- [5] H.P. Kim, et al., Sensing mechanism of SnO₂-based sensors for alcohols, *Sens. Actuators B Chem.* 14 (1–3) (1993) 511–512.
- [6] L. Promsong, M. Sriyudthsak, Thin tin-oxide film alcohol-gas sensor, *Sens. Actuators B Chem.* 25 (1–3) (1995) 504–506.
- [7] G. Sberveglieri, et al., A novel PVD technique for the preparation of SnO₂ thin films as C₂H₅OH sensors, *Sens. Actuators B Chem.* 7 (1–3) (1992) 721–726.
- [8] T. Zhang, Y. Shen, R. Zhang, Ilmenite structure-type [beta]-CdSnO₃ used as an ethanol sensing material, *Mater. Lett.* 23 (1–3) (1995) 69–71.
- [9] Y. Chen, K.Y. Chen, A.C.C. Tseung, An electrochemical alcohol sensor based on a co-electrodeposited Pt|WO₃ electrode, *J. Electroanal. Chem.* 471 (2) (1999) 151–155.
- [10] G. Sberveglieri, et al., Sol-gel prepared nanosized TiO₂ thin films for alcohol sensing, in: *Proceedings of the Transducers '99, 10th International Conference on Solid-State Sensors and Actuators*, Sendai, Japan, 1999.
- [11] S. Zhao, et al., A high performance ethanol sensor based on field-effect transistor using a LaFeO₃ nano-crystalline thin-film as a gate electrode, *Sens. Actuators B Chem.* 64 (1–3) (2000) 83–87.
- [12] E. Comini, et al., Sensitivity enhancement towards ethanol and methanol of TiO₂ films doped with Pt and Nb, *Sens. Actuators B Chem.* 64 (1–3) (2000) 169–174.
- [13] P. Ramesh, S. Sampath, A binderless, bulk-modified renewable surface amperometric sensor for NADH and ethanol, *Anal. Chem.* 72 (14) (2000) 3369–3373.
- [14] I.T. Weber, E. Longo, E. Leite, SnO₂·Nb₂O₅ films for ethanol sensor, obtained by deposition of alcoholic suspensions, *Mater. Lett.* 43 (4) (2000) 166–169.
- [15] Y.F. Dong, W.L. Wang, K.J. Liao, Ethanol-sensing characteristics of pure and Pt-activated CdIn₂O₄ films prepared by r.f. reactive sputtering, *Sens. Actuators B Chem.* 67 (3) (2000) 254–257.
- [16] S. Tao, et al., Ethanol-sensing characteristics of barium stannate prepared by chemical precipitation, *Sens. Actuators B Chem.* 71 (3) (2000) 223–227.
- [17] O.K. Tan, et al., Size effect and gas sensing characteristics of nanocrystalline xSnO₂-(1-x)[alpha]-Fe₂O₃ ethanol sensors, *Sens. Actuators B Chem.* 65 (1–3) (2000) 361–365.
- [18] I.T. Weber, et al., A study of the SnO₂·Nb₂O₅ system for an ethanol vapour sensor: a correlation between microstructure and sensor performance, *Sens. Actuators B Chem.* 72 (2) (2001) 180–183.
- [19] C.-C. Pang, et al., An amperometric ethanol sensor by using nickel modified carbon-rod electrode, *Sens. Actuators B Chem.* 73 (2–3) (2001) 221–227.
- [20] F. Gao, Y. Liu, X. Liu, The catalytic effects of the Mg²⁺-doping on the ethanol-sensing properties of Cd₂Sb₂O_{6.8}, *Sens. Actuators B Chem.* 77 (3) (2001) 653–656.
- [21] C.V. Gopal Reddy, et al., Preparation of Fe₂O₃(0.9)-SnO₂(0.1) by hydrazine method: application as an alcohol sensor, *Sens. Actuators B Chem.* 81 (2–3) (2002) 170–175.
- [22] C. Garzella, et al., Sol-gel TiO₂ and W/TiO₂ nanostructured thin films for control of drunken driving, *Sens. Actuators B Chem.* 83 (1–3) (2002) 230–237.
- [23] G. Jin, et al., Polypyrrole filament sensors for gases and vapours, *Curr. Appl. Phys.* 4 (2–4) (2004) 366–369.
- [24] K.M. Lee, et al., Volatile organic gas recognition using conducting polymer sensor array, in: *Eco-Mater. Process. Des.*, 2003, pp. 344–351.
- [25] Y.G. Lee, T.C. Chou, Nickel-based thick film ethanol sensor, *Electroanalysis* 15 (20) (2003) 1589–1597.
- [26] A. Pich, et al., Thermo-sensitive poly(*N*-vinylcaprolactam-co-acetoacetoxyethyl methacrylate) microgels 3. Incorporation of polypyrrole by selective microgel swelling in ethanol–water mixtures, *Polymer* 45 (4) (2004) 1079–1087.
- [27] G.J. Mohr, et al., Fluorescent ligands for optical sensing of alcohols: synthesis and characterisation of *p*-*N,N*-dialkylamino-trifluoroacetylstilbenes, *Anal. Chim. Acta* 344 (3) (1997) 215–225.
- [28] G.J. Mohr, D. Citterio, U.E. Spichiger-Keller, Development of chromogenic reactants for optical sensing of alcohols, *Sens. Actuators B Chem.* 49 (3) (1998) 226–234.
- [29] Z. Zhang, C. Zhang, X. Zhang, Development of a chemiluminescence ethanol sensor based on nanosized ZrO₂, *Analyst* 127 (6) (2002) 792–796.
- [30] G.J. Mohr, Tailoring the sensitivity and spectral properties of a chromoreactant for the detection of amines and alcohols, *Anal. Chim. Acta* 508 (2) (2004) 233–237.
- [31] G.J. Mohr, New chromoreactants for the detection of aldehydes, amines and alcohols, *Sens. Actuators B Chem.* 90 (1–3) (2003) 31–36.
- [32] P. Blum, et al., Optical alcohol sensor using lipophilic Reichardt's dyes in polymer membranes, *Anal. Chim. Acta* 432 (2) (2001) 269–275.
- [33] F.L. Dickert, M. Keppler, Self-organized phases combined with IDC devices—switchable materials for solvent vapor detection, *Adv. Mater.* 7 (12) (1995) 1020–1023.
- [34] M.C. Lonergan, et al., Array-based vapor sensing using chemically sensitive, carbon black-polymer resistors, *Chem. Mater.* 8 (9) (1996) 2298–2312.

- [35] M. Riepl, et al., Optimization of capacitive affinity sensors: drift suppression and signal amplification, *Anal. Chim. Acta* 392 (1) (1999) 77–84.
- [36] F. Josse, et al., AC-impedance-based chemical sensors for organic solvent vapors, *Sens. Actuators B-Chem.* 36 (1–3) (1996) 363–369.
- [37] A. Hierlemann, et al., CMOS-based chemical microsensors: components of a micronose system, in: *Proceedings of the SPIE—The International Society for Optical Engineering* 3857, 1999, pp. 158–169.
- [38] C. Hagleitner, et al., CMOS single-chip gas detection system comprising capacitive calorimetric and mass-sensitive microsensors, *IEEE J. Solid State Circuits* 37 (12) (2002) 1867–1878.
- [39] S.-J. Kim, et al., Capacitive porous silicon sensors for measurement of low alcohol gas concentration at room temperature, *J. Solid State Electrochem.* 4 (6) (2000) 363–366.
- [40] S.V. Patel, et al., Chemicapacitive microsensors for volatile organic compound detection, *Sens. Actuators B Chem.* 96 (3) (2003) 541–553.
- [41] G.Y. Chen, et al., Adsorption-induced surface stress and its effects on resonance frequency of microcantilevers, *J. Appl. Phys.* 77 (8) (1995) 3618–3622.
- [42] H.P. Lang, et al., A chemical sensor based on a micromechanical cantilever array for the identification of gases and vapors, *Appl. Phys. A (Mater. Sci. Process.)* 66 (Suppl. Part 1–2, Part 1–2) (1998) S61–S64.
- [43] M.K. Baller, et al., A cantilever array-based artificial nose, *Ultramicroscopy* 82 (1–4) (2000) 1–9.
- [44] F.M. Battiston, et al., A chemical sensor based on a microfabricated cantilever array with simultaneous resonance-frequency and bending readout, *Sens. Actuators B Chem.* 77 (1–2) (2001) 122–131.
- [45] A. Boisen, et al., Environmental sensors based on micromachined cantilevers with integrated read-out, *Ultramicroscopy* 82 (1–4) (2000) 11–16.
- [46] B.C. Fagan, et al., Modification of micro-cantilever sensors with sol-gels to enhance performance and immobilize chemically selective phases, *Talanta* 53 (3) (2000) 599–608.
- [47] H. Jensenius, et al., A microcantilever-based alcohol vapor sensor-application and response model, *Appl. Phys. Lett.* 76 (18) (2000) 2615–2617.
- [48] D. Lange, et al., Complementary metal oxide semiconductor cantilever arrays on a single chip: mass-sensitive detection of volatile organic compounds, *Anal. Chem.* 74 (13) (2002) 3084–3095.
- [49] J.D. Adams, et al., Nanowatt chemical vapor detection with a self-sensing, piezoelectric microcantilever array, *Appl. Phys. Lett.* 83 (16) (2003) 3428–3430.
- [50] E.A. Wachter, et al., Remote optical detection using microcantilevers, *Rev. Sci. Instrum.* 67 (10) (1996) 3434–3439.
- [51] K.M. Hansen, et al., Cantilever-based optical deflection assay for discrimination of DNA single-nucleotide mismatches, *Anal. Chem.* 73 (7) (2001) 1567–1571.
- [52] M. Sepaniak, et al., Microcantilever transducers: a new approach to sensor technology, *Anal. Chem.* 74 (21) (2002) 568A–575A.
- [53] L. Manning, et al., Self-oscillating tapping mode atomic force microscopy, *Rev. Sci. Instrum.* 74 (9) (2003) 4220–4222.
- [54] P.G. Datskos, T. Thundat, Nanocantilever signal transduction by electron transfer, *J. Nanosci. Nanotechnol.* 2 (3–4) (2002) 369–373.
- [55] X.M. Yu, et al., Noise and sensitivity in polysilicon piezoresistive cantilevers, *Chin. Phys.* 10 (10) (2001) 918–923.
- [56] L.A. Pinnaduwa, et al., Adsorption of trinitrotoluene on uncoated silicon microcantilever surfaces, *Langmuir* 20 (7) (2004) 2690–2694.
- [57] C.L. Britton, et al., Multiple-input microcantilever sensors, *Ultramicroscopy* 82 (1–4) (2000) 17–21.
- [58] D.R. Baselt, et al., Design and performance of a microcantilever-based hydrogen sensor, *Sens. Actuators B Chem.* 88 (2) (2003) 120–131.
- [59] A. Mehta, et al., Manipulation and controlled amplification of Brownian motion of microcantilever sensors, *Appl. Phys. Lett.* 78 (11) (2001) 1637–1639.
- [60] P. Dutta, et al., Enantioselective sensors based on antibody-mediated nanomechanics, *Anal. Chem.* 75 (10) (2003) 2342–2348.
- [61] G. Delapierre, et al., Polymer-based capacitive humidity sensor: characteristics and experimental results*1, *Sens. Actuators* 4 (1983) 97–104.
- [62] H. Shibata, et al., A digital hygrometer using a polyimide film relative humidity sensor, *IEEE Trans. Instrum. Meas.* 45 (2) (1996) 564–569.
- [63] S.G. Davila, R.S.F. Silva, Isothermal vapor–liquid equilibrium data by total pressure method—systems acetaldehyde–ethanol, acetaldehyde–water, and ethanol–water, *J. Chem. Eng. Data* 15 (3) (1970) 421–424.
- [64] J. Gmehling, U. Onken, *Vapor–Liquid Equilibrium Data Collection*, vol. 1, Verlag, Rankfurt, Germany, 1977.
- [65] J. Gmehling, U. Onken, W. Arlt, *Vapor–Liquid Equilibrium Data Collection*, vol. 1a, Schon & Wetzels, Frankfurt, Germany, 1981.
- [66] T.L. Ferrell, et al., Telesensor integrated circuits, *World J. Surg.* 25 (11) (2001) 1412–1418.
- [67] <http://www.osmolabstore.com>.
- [68] J.W. Crate, M.H. Abraham, R.A. McGill, Sorbent polymer materials for chemical sensors and arrays, in: E. Kress-Rogers (Ed.), *Handbook of Biosensors and Electronic Noses*, CRC Press, Boca Raton, 1997, pp. 593–612.
- [69] G. Harsanyi, *Polymer Films in Sensor Applications*, Technomic Publishing Co., Lancaster, Pennsylvania, 1995.
- [70] R.A. McGill, E.J. Houser, T.E. Mlsna, Linear and branched chemoselective siloxane polymers and methods for use in analytical and purification applications, United States Patent, USA, 2003.
- [71] D.R. Lide, *Handbook of Chemistry and Physics*, CRC Press, Boca Raton, FL, 1995, pp. 6–10.